European Journal of Molecular & Clinical Medicine

ISSN 2515-8260 Volume 08, Issue 03, 2021

Convolutional Neural Network Architecture for Skin Cancer Diagnosis

Michael Cabanillas-Carbonell
Facultad de Ingeniería
Universidad Privada del Norte
Lima, Perú
0000-0001-9675-0970

Randy Verdecia-Peña
ETSI de Telecomunicación
Universidad Politécnica de Madrid
Madrid, Spain
0000-0003-4798-2681

Abstract*— In recent years, Malignant Melanoma Cancer has caused an increased exponential in human diseases, for this reason, it is essential to detect it from its early stages. Deep Learning is one of the most applied technologies for the analysis of images oriented to medicine, facilitating the diagnosis of diseases in patients, allowing them to make accurate decisions about their health. In this paper, we propose a convolutional neural network architecture derived from the evaluation of different convolutional neural networks that meet the objective of obtaining more pressure on the information of the acquired image. The model for the problem is based on a binary distribution, 1 in case of malignant and 0 for benign, so that melanoma can be detected early and is very useful, for this we used 2 different datasets with a total of 2650 images for training the architecture. Finally, a comparison of the results obtained in other research has been made, where the metrics of our project are considerably improved by having 3 layers. This new architecture is a proposed solution for the optimization of training and validation of images.

***Keywords*— skin cancer, melanoma, neural network, deep learning**

I. INTRODUCTION

The skin is the largest organ in the human body that fulfills the function of protecting the internal parts of the human body from the outside, being one of the most important organs Skin cancer is considered one of the most dangerous cancers, due to the increasing incidence of this disease, which can develop in any part of the body. There are two types of these tumors, malignant and benign; the most prominent and the one that has been increasing for the last 30 years is malignant melanoma [1]. According to Cancer Statistics, 100,350 new cases of melanoma were estimated to be diagnosed in the United States in 2020 alone, compared to 2019 when 96,480 cases were estimated [2], [3]. The Melanoma Research Foundation (MRF) mentions that melanomas are considered 90% preventable, and may be treatable when detected early, and are considered to have a high survival [4].

In Peru, approximately 1,200 new patients with skin cancer are detected each year; in addition, 500 people die each year as a result of melanoma [5]. In Reference [6], shows the results of the analysis of the cancer situation in Peru, it was possible to identify that between the years 2014 – 2018, skin cancer was the third most frequent type of cancer, accounting for 10.8% of the total population.

Early detection, restaging and treatment are critical for melanoma therapy and can help save more than 95% of people [5]. Self-examination improves the likelihood of early diagnosis helping to reduce mortality by 63%, however, only less than 25% of patients perform skin self-examination [2].

The persistent increase of this type of cancer, the high medical cost and the high mortality rate have given way to the prioritization of early diagnosis of this cancer. Anticipation and cure of melanoma is strictly relevant, if it is identified prematurely, the survival rate will increase [1].

Dermatoscopy is one of the most important techniques for examining skin lesions and can capture high-resolution images of the skin that escape the disruption of surface reflections. Specially trained physicians use this high-resolution imaging to assess the possibility of melanoma early on and can obtain a diagnostic accuracy as high as 80%; however, there are not enough experienced dermatologists worldwide [7].

Early diagnosis of this cancer is very important for two reasons, firstly, the diagnosis of skin cancer is accessible due to its external location and secondly early identification of melanoma is of utmost importance to help determine its thickness. In early stages where the thickness is below 1 mm, melanoma can be successfully eradicated. However, melanoma is complicated to identify in the early stages, even by experienced specialists in the field [8].

In 2017, a research has been developed which focuses on detecting skin cancer based on a deep learning model [9]. For this reason, the aim is to improve these values using a convolutional neural network by creating a new model. Therefore, motivated by the above issues, in this paper, we developed Deep Learning prototype based on image analysis to detect whether it is malignant or benign cancer using dermoscopy image databases in the academic research community.

The purpose of this work is to demonstrate that skin cancer diagnosis can be performed by Deep Learning in a reliable and effective way, using a new architecture proposed in this paper. To achieve this demonstration, empirical tests were performed on skin cancer image databases. The analysis of these images will allow for extensive training and validation to classify as malignant or benign.

The article is divided into sections, where Section II details the theoretical foundation where basic concepts about skin cancer and the technology to be implemented are provided, Section III details the methodology to be implemented and its development; Section IV details the results obtained and Section V the conclusions and future work. Finally, the references are found.

II. THEORETICAL FOUNDATION

The skin is characterized by 3 layers epidermis, dermis and subcutaneous cellular tissue. The epidermis is the outer layer of the skin, the dermis lies beneath the epidermis and exceeds it in thickness, and the subcutaneous cellular tissue lies beneath the dermis and contains collagen fibers and fat cells[10].

These cells divide continuously in a programmed and controlled manner to form new cells and replace those that have been aging and dying. This generates a balance in the production of new cells and the elimination of dead cells, allowing the skin to function in a balanced way. When this balance is lost, caused by mutations in the genes, uncontrolled growth and excessive division of a certain type of cell occurs, leading to cancer. In general, skin cancer is divided into benign and malignant melanoma [11].

Diagnosis of skin tumors begins with the physician's clinical examination of the lesion with the naked eye. This examination is usually accompanied by dermoscopic examination, a noninvasive technique that allows the exploration of suspicious lesions and tumors, providing a very accurate diagnosis [12]. One influencing factor is characteristics that can possibly affect the causes of disease, in this case, skin cancer. Each type of cancer has different risk factors. Some risk factors, such as sun exposure, can be controlled [12]. Others, such as personal history, age or genetic characteristics, cannot be modified.

A. Artificial Neural Network

Artificial Neural Networks are those networks in which there are information processing elements, which perform local interactions and these depend on the behavior of the whole system trying to simulate the behavior of the human brain [6]. These systems simulate in a schematic way the neuronal structure of the brain, through a computer program by means of the physical construction of systems whose architecture approximates the structure of the biological neuronal network.

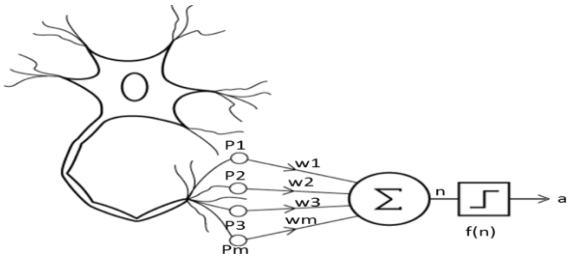

Fig.1. Structures of an artificial neuron system [13]

B. Convolutional neural network

A Convolutional Neural Network (CNN) is an analog of traditional artificial intelligence because they are made up of neurons that self-optimize through learning. As shown in Fig. 2, each neuron will receive an input and perform a scalar product operation followed by a nonlinear function, based on the innumeracy of artificial intelligence. From the input raw image vectors to the final output in scoring for the class, the whole network will continue to express a single prescriptive scoring function to the weight so that they can get the best accuracy of the image taken [14].

For digit recognition it is necessary to introduce two layers that define convolutional networks, which can be expressed as groups of neurons specialized in two operations: convolution and pooling [15].

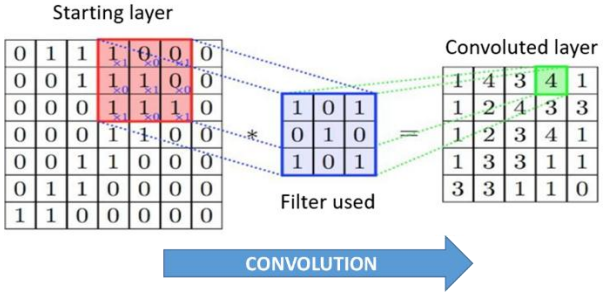

Fig. 2. Example of convolution [16].

1) Convolution operation: The output of the neurons will be arranged by convolution, classifying those that are connected to local regions of the input by calculating the producing scalar between their weights and the region linked to the input volume. The rectified linear unit called ReLu aims to superimpose an element-wise activation function, such as sigmoid, on the activation output produced by the previous layer [15].

2) Pooling operation: The pooling layer is the one that performs down-sampling along the size of the spatial dimension of the input provided, further reducing the number of parameters within that activation [14].

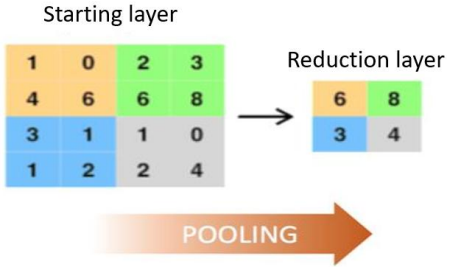

Fig. 3. Example of reduction [16].

3) Fully connected layers: They perform the same tasks that are localized in ANNs and will try to produce class scores from activations for use in the distribution, along with ReLu between these layers, to improve performance [17].

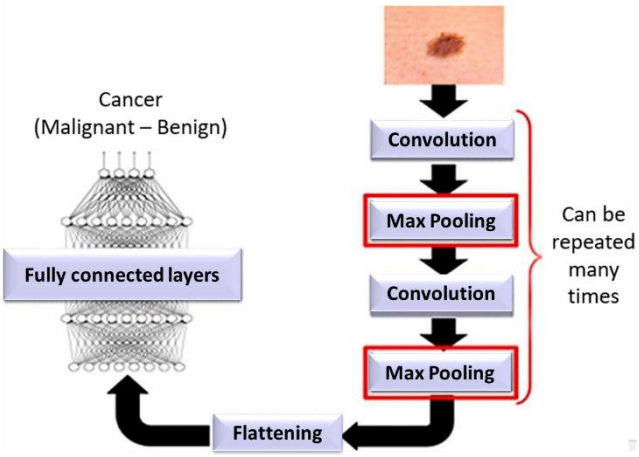

Fig. 4. Fully connected layers [18].

The operation of a convolutional neural network has two components [18]:

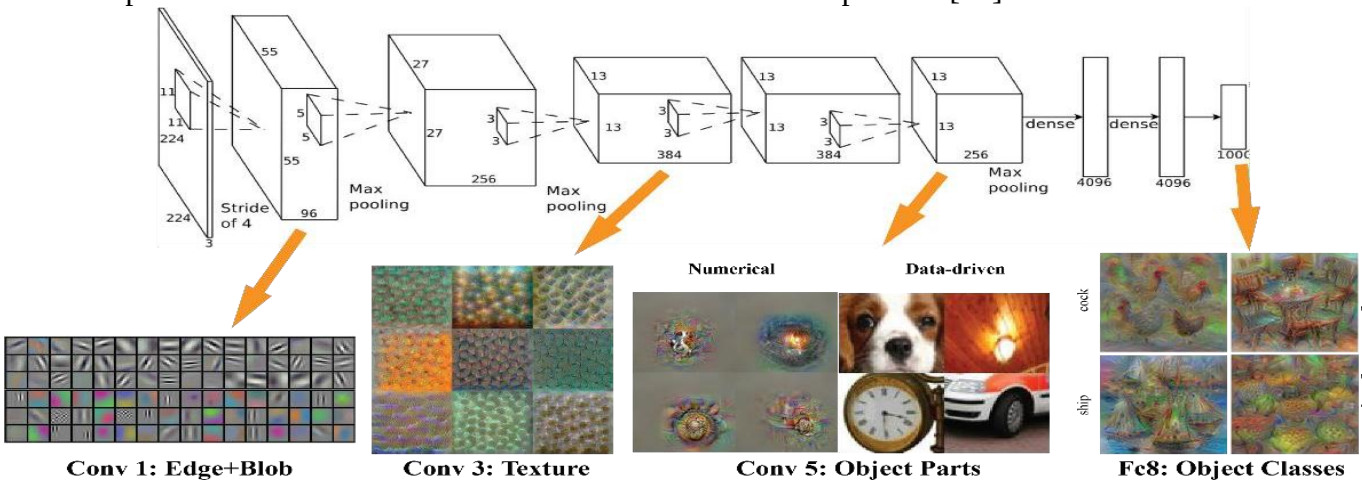

Fig. 5. Operation of a CNN [19].

a) Hidden layers: In this part, the network will perform a series of convolutions and pooling operations during which features are detected.

b) Classifier: Here, the fully connected layers will serve as a classifier on top of these extracted features.

C. Padding:

It allows us to conserve the size of the input matrix, in order to use deep neural networks, we really need to use padding. To give you a rule of thumb, if a filter $n * n$ is applied to a matrix fxf, we have $(n - f + 1)x(n - f + 1)$.

The convolution operation reduces the matrix if $f > 1$, if we want to apply the convolution operation several times, but if the image is reduced, we will lose a lot of data in this process. In almost all cases the padding values are zeros. The general rule now, if a matrix nxn is applied a filter of $fxff$ and a padding p, this gives us a matrix [19].

$$(n - 2p + f + 1)\ x\ (n - 2p - f + 1)$$

D. Stride

Controls how the filter advances over the input volume. Calculating the stride of a matrix nxn we apply a filter of $f * f$ and a padding p, and give a stride s, we have the following matrix.

$$\frac{n + 2p - f}{s} + 1x\frac{n + 2p - f}{s} + 1$$

E. *Python*

It is an interpreted programming language where it is based on a syntax that favors a readable and clean code, since it is versatile cross-platform and multi-paradigm [20].

III. METHODOLOGY

For the development of this project a deep study was carried out in the field of learning about the impact of skin image by image classification. In order to achieve the objective of the project has been adopted by the proposal of a convolutional network architecture of image classification.

The methodology to be used is descriptive in nature, and consists of finding out predominant attitudes, situations and customs that can accurately describe the activities, using data collection, analysis and interpretation techniques.

A. *Case Study*

The case study was carried out based on the interpretation of the data evaluated in terms of the accuracy of the techniques analyzed. In this case, databases concerning skin cancer were evaluated where images available in public internet repositories were obtained.

B. *Observation techniques and data collection instruments*

The confusion matrix was used which will allow us to see the performance of the model to differentiate between malignant and benign.

C. *Datasets*

Two repositories were used for this work, the first set of images with ISBI nomenclature, ISIC_UDA-2_1 and ISIC_MSK-1_1 for skin cancer analysis are from the ISIC Arhcive repository with a total of 2650 images [21], the second set of images with IMD nomenclature were obtained from the PH2Dataset repository with a total of 200 images, these images are validated by Pedro Hispano Hospital [22]. The dataset is publicly available; all images are labeled as benign or malignant and included to label the lesion within the image. For the image set, it was distributed as follows:

- Use a zero before. Image segmentation. The image set is divided into 60% training, 20% validation and 20% test images, this was performed by the two image sets separately and together.
- Image classification. Exclude images with altered or blurred lesions.

D. *Neural network architecture*

Nowadays, there are several convolutional neural network architectures such as ImageNet Large Scale visual recognition, which became very popular in deep learning. There are several image classification architectures such as VGG-16, AlexNet and GoogleNet, our purpose is to propose an architecture for skin cancer recognition.

1) Proposed neural network: An input image is taken for CNN's image classifications, processed and organized according to its category criteria. Computers see an image as a matrix of pixels and depending on the resolution of the image, it will look like H x W x D, where H is the height, W is the width and D is the dimension.

For the project our images were based on the RGB type (chromatic model from the mixture of 3 primary colors), where the input images were 150 x 150 x 3, the value 3 refers to the RGB values. Then the values are reflected as follows:

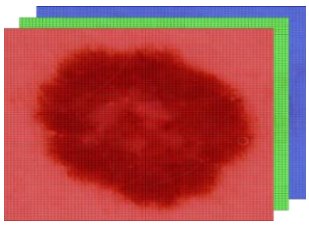

Fig. 6. RGB matrix 150 x 150 x 3.

After defining the dimensions of the input image, the next step is to define the convolution, which is the first layer that extracts properties from an input image. The convolution performed safeguards the relationship between pixels by learning the image features using small input data frames. Fig. 7 shows the mathematical procedure that receives two inputs such as an image matrix and a filter.

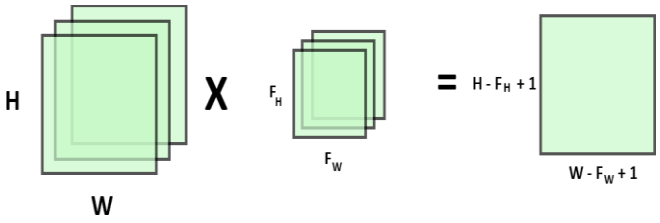

Fig. 7. RGB matrix multiplies the filter matrix.

Then considering convolution, we replace the values of the 150 x 150 input image whose image pixels are 0 and 1; and a 3 x 3 filter matrix as shown below:

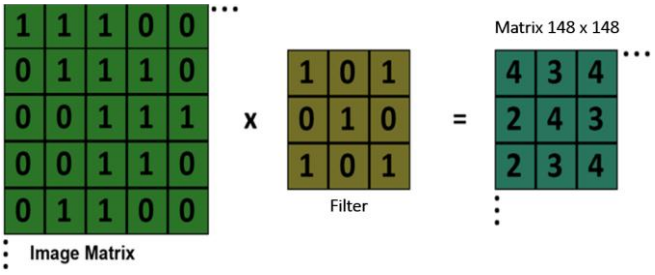

Fig. 8. Output matrix 148 x 148.

The convolution of the images when performing the different filters can find edge detection, blur and sharpness. The stride or displacement is 1, i.e. the filter will advance 1 by 1 at a time.

Next, a 148 x 148 matrix was obtained with a depth filter of 32, to which an activation function was applied, in this case we will use the function.

ReLu, as it guarantees better performance over sigmoid in image classification. The purpose of ReLu is to introduce nonlinearity in our convolutional neural network.

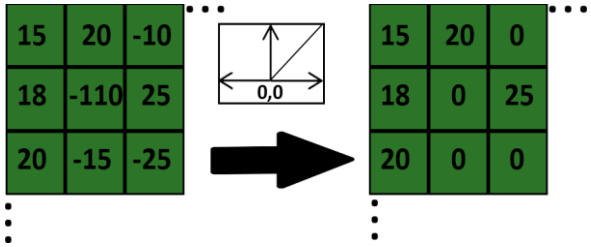

Fig. 9. Operation ReLu to CNN.

Now, the next thing will be to reduce the number of parameters, for this we will use the Max Pooling grouping, where it takes the largest element or the most important characteristic. Then our matrix will look like this applying a Max Pool of 2 x 2 and a default stride of 2:

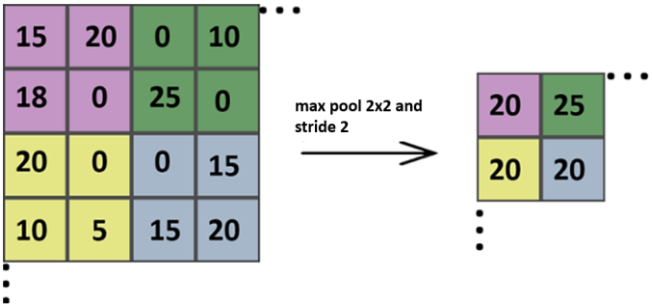

Fig. 10. Max pooling 2x2 grouping.

Here we conclude with the convolution, adding convolutional layers and pooling layers until the neural network obtains the best characteristics and stop adding more convolutions until it starts to obtain other characteristics. Once this process is completed, we will equalize the matrix in a vector and feed it into a fully connected layer that will be our neural network using the Backpropation algorithm, this would be represented as follows.

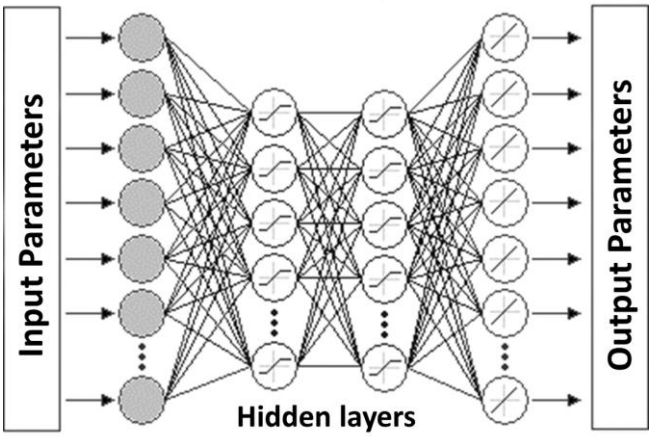

Fig. 11. Fully connected layers.

In Fig. 11, it shows us that 64 neurons enter as parameters, these were sent to a vector where it finally gave other output parameters. We will perform this process once again, but we will tell it to do it to a single neuron, this serves us to obtain only 1 response.

Finally, we have an activation function as softmax or sigmoid, which our case will be sigmoid to classify the image as malignant or benign cancer.

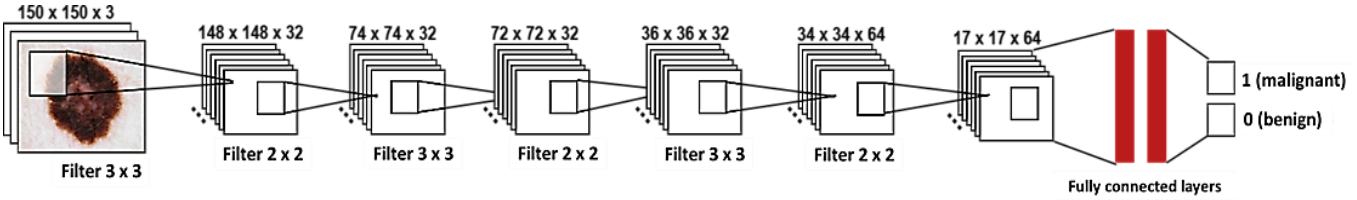

Fig. 12. Proposed architecture.

Fig. 12 shows that the architecture is based on a sequential model, in which the input layer is of RGB type, passing the images through three convolutional blocks, using small 3 by 3 filters, including a 2D convolution operation for each block and swapping between them. The activation function layer as well as the other layers are equipped with a ReLu, being a nonlinearity operation and including spatial clustering through the use of a maximum clustering layer. This network ended with a classifier block that consists of a single layer. When the final output layer is fully connected, it performs a binary categorization and a sigmoid activation function.

E. Data augmentation

The data magnification techniques selected were: resizing, 255-degree rotation, horizontal shift, and image zoom. In addition, data augmentation also helped to prevent over-fitting, helping to balance the datasets to generate the same number of images to compare the results.

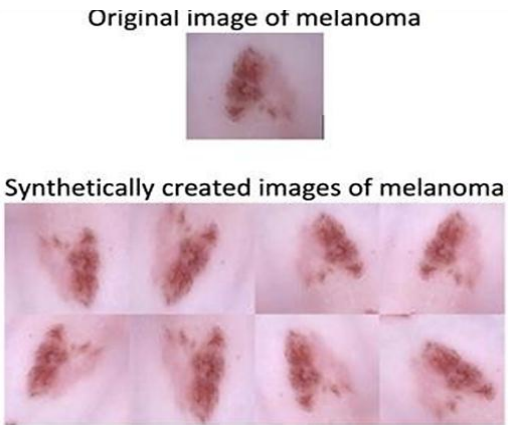

Fig. 13. Data augmented malignant imaging [23].

F. Training method

The training methodology is the most suitable to help us provide a solution to the above-mentioned problem. Focusing on the diagram proposed in Fig. 14, it is shown that the training of the data was performed through the learning algorithm defined by each model, applying stochastic gradient descent. After the algorithm has been trained and has learned the weights, the classification of the validation data is performed by means of a prediction algorithm. Finally, the model is evaluated by comparing the predictions with the basic data.

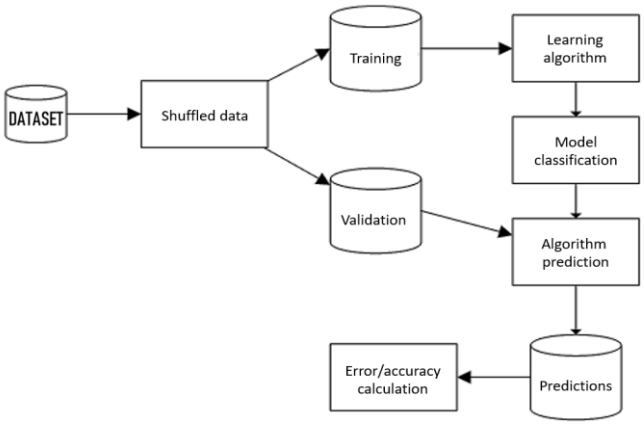

Fig. 14. Training methodology

IV. ANALYSIS OF RESULTS

The following training sessions were conducted:

- First, the ISIC dataset was used to perform the training and validation performed by the proposed model.
- Second, the PH2 dataset was used to perform the training and validation performed by the proposed model.
- Third, the two datasets were merged by performing the training and validation performed by the proposed model.

The training was performed according to the parameters chosen for the classification process which were 100 epochs chosen based on the examination of the behavior of the accuracy/loss vs. number of epochs graphs, where each epoch took 300 seconds of the GPU (Graphics Processing Unit). The tuning process was performed with a very small learning rate, helping to minimize the loss function of the Adam optimizer.

A. Metrics

The main metrics used for the evaluation of this work were as follows**:**

1) Accuracy: Calculate the number of correct predictions divided by the total number of samples.

$$Accuracy = \frac{Nº\ correct\ predictions}{Nº\ examples}$$

2) Sensitivity: It is calculated as the proportion of times a result shows true positives. The closer the sensitivity is to 100%, the more likely it is that a patient has a disease.

$$Sensitivity = \frac{Nº\ true\ positives}{Nº\ true\ positives + Nº\ false\ negatives}$$

3) Precision: It is calculated as the fraction of retrieved instances that are relevant.

$$Precision = \frac{Nº\ true\ positives}{Nº\ true\ positives + Nº\ \ false\ positives}$$

4) Specificity: It is calculated as the proportion of the time in which a result gives true negatives. As specificity approaches 100% it is more likely that a result means that the patient does not have a disease.

$$Especificidad = \frac{Nº\ \ true\ negative}{Nº\ true\ negative\ \ + \ Nº\ false\ positive}$$

B. Training

For training, a convolutional layer had to be added first, to find the best results, on the layer with the highest accuracy. Fig. 15 shows the accuracy values based on the PH2.

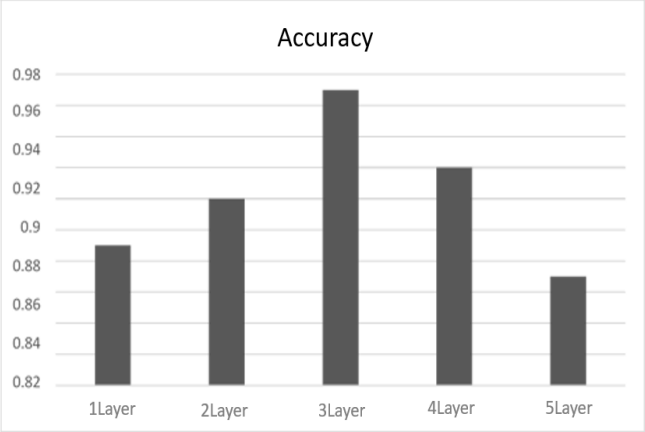

Fig. 15. Results with different convolutional layers.

The following precision and recovery metrics were obtained.

TABLE I. PRECISION METRICS AND LAYERED RECOVER

Layer	Recall	F1 Score	Precision
1	0.853174	0.844792	0.836575
2	0.903113	0.898136	0.893215

Layer	Recall	F1 Score	Precision
3	0.970011	0.971652	0.973300
4	0.910789	0.916138	0.921553
5	0.811363	0.834938	0.859926

The F1-Score metric seeks a balance between accuracy and recovery, so in the table we can see that the accuracy in layer 3, F1-Score indicates that we have a good accuracy and recovery in this layer. From there, we can perform the training using the architecture with layer 3, the architectures can be seen in Annex B.

The training results are based on an automatically created binary calculation. Let's obtain the average of the probabilities obtained by our neural network in training.

The results obtained from the dataset, according to the metrics according to the tests performed on layer 3, were as follows:

TABLE II. COMPARISON OF TRAINING METRICS BY DATASET

Dataset	Accuracy	Sensitivity	Specificity	Precision
DATASET ISIC	0.8887	0.8322	0.9681	0.9735
DATASET PH2	0.9250	0.9047	0.9473	0.9500
DATASET JUNTO	0.8982	0.8626	0.9747	0.9473

We compared the results with the two data sets separately and together as shown in Table 2, what we want to achieve with these results is to see the performance of each data set separately.

In Fig. 16, the images of the training to diagnose malignant or benign cancer are shown, we can see that there is a great closeness between the error and the true even though the image is clear and sharp. This is an example of the operation of the convolutional neural network already trained, finally it will give us the result of benign or malignant, there is no internal detail of how the process is performed, because in neural networks the parameters and processing is done internally.

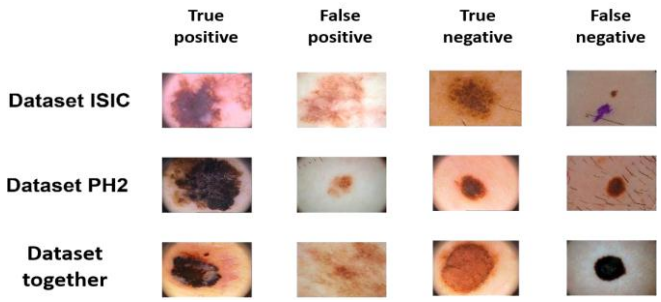

Fig. 16. Benign image.

Finally, it shows the ROC curve to evaluate the binary classification performance.

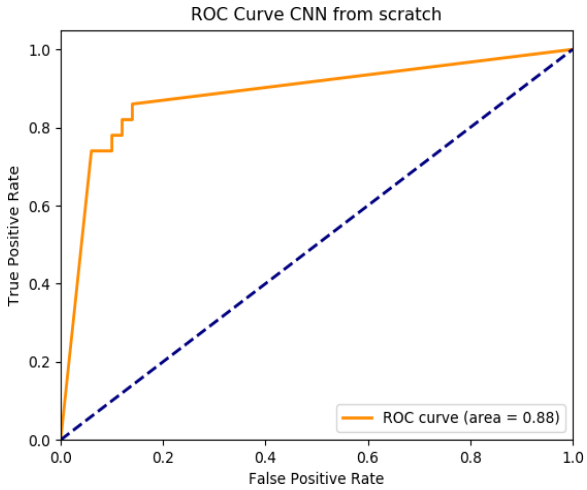

Fig. 17. ROC curve for ISIC dataset.

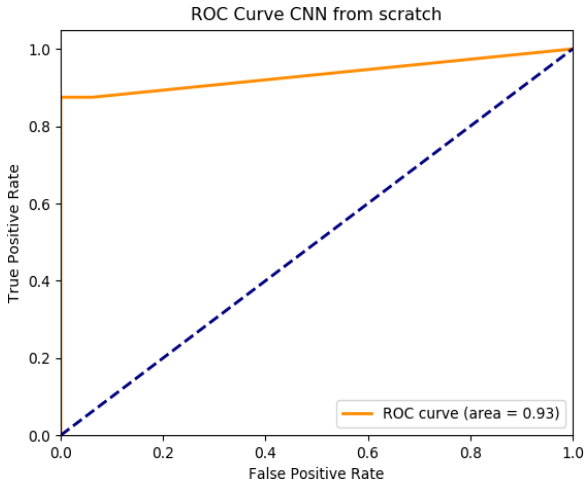

Fig. 18. ROC curve for dataset PH2.

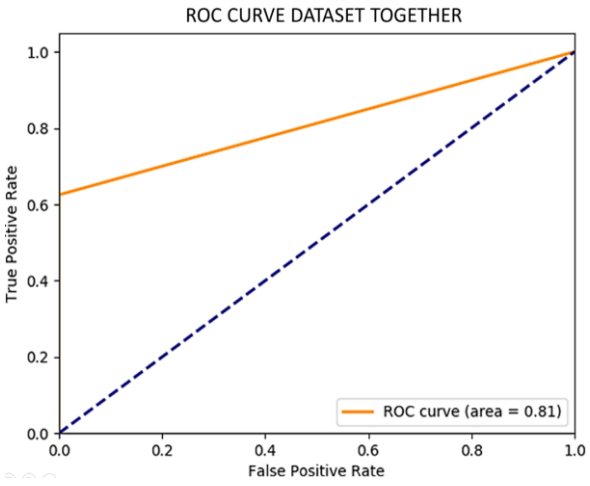

Fig. 19. ROC curve for dataset together.

We can visualize that in our three cases the ROC curve represents the sensitivity versus specificity to classify into malignant and benign cancer, seeing that our network found a higher amount of true positives to false positives, this means that the threshold can classify the dermoscopic images. This implies that the proposed model can generalize well to a wide variety of classification problems, even with images that are not found in the dataset.

C. Validation

The results of this model demonstrate that good performance can be obtained by proposing the originally trained architecture for dataset image classification. This implies that the proposed model can generalize well to a wide variety of classification problems, even with images not found the dataset.

The confusion matrix is represented in the following tables, which show the classification performance of the model in dataset validation. It should be considered that the evaluation of the model is related to the number of true melanomas considered as benign cases. Here the incorrect case is presented, where the model does not detect a real case of melanoma putting the patient at risk.

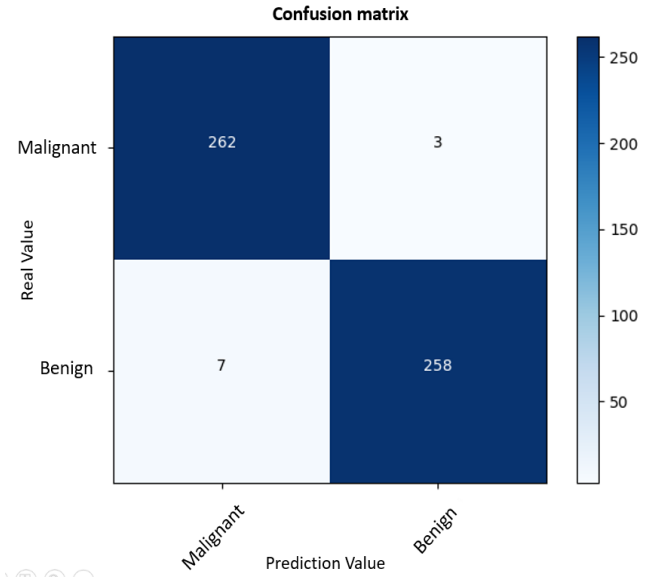

Fig. 20. Representation of the ISIC confusion matrix

It can be observed in the confusion matrix that 265 malignant and 265 benign images were entered. Where 262 images were correctly predicted and 3 were classified as benign, and in the case of benign images 7 were classified as malignant and 258 as benign.

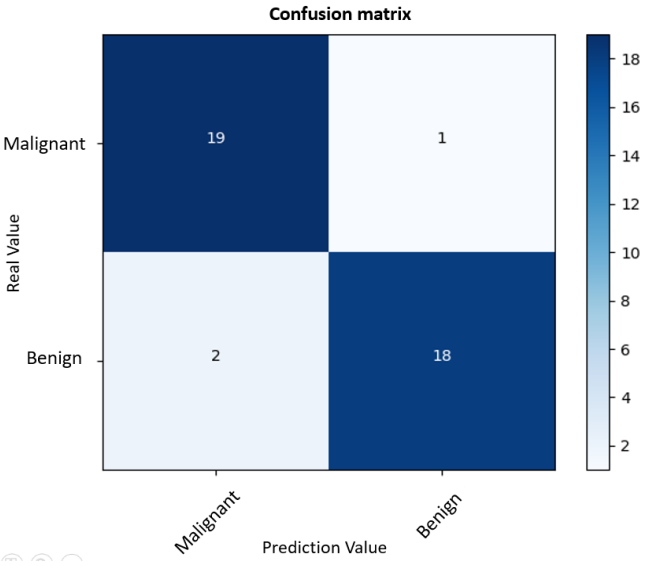

Fig. 21. Representation of the confusion matrix PH2.

It can be observed in the confusion matrix that 20 malignant and 20 benign images were entered. Where 19 images were correctly predicted and 1 was classified as benign, and in the case of benign images 2 were classified as malignant and 18 as benign.

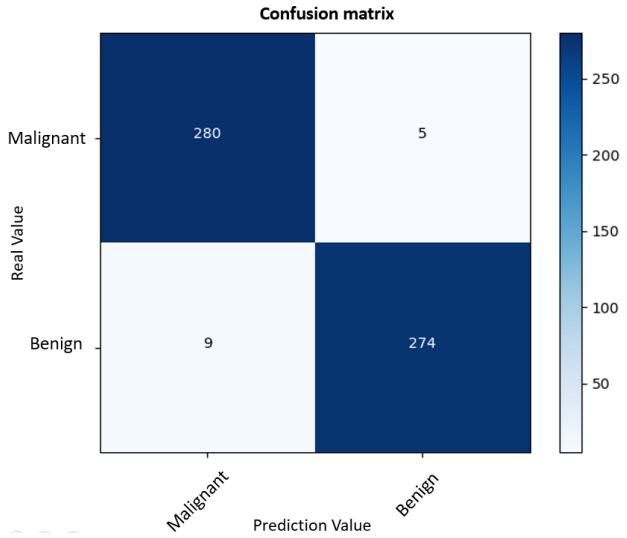

Fig. 22. Representation of the confusion matrix TOGETHER

It can be observed in the confusion matrix that 285 malignant and 285 benign images were entered. Where 280 images were correctly predicted and 5 were classified as benign, and in the case of benign images 9 were classified as malignant and 274 as benign.

Comparison with the ISIC dataset of our project and with the project of the reference [24], because this project uses the same dataset, with the VGG-16 architecture.

TABLE III. COMPARISON OF VALIDATION METRICS WITH OTHER PROJECTS

Project	Accuracy	Lost	Sensitivity	Precision
Proyecto Dataset ISIC	0.8887	0.1910	0.8322	0.9735
Skin Lesion Detection CNN	0.8390	0.4723	0.8243	0.9523

V. CONCLUSIONS AND FUTURE WORK

This proposed Deep Learning neural network was made to achieve excellent performance on the set of analyzed images, providing help to physicians and patients for the diagnosis of skin lesions. The tool helps to detect in malignant or benign cancer, using the convolutional neural network for early classification of melanoma.

For the proposal, each of the datasets was analyzed separately, to obtain the performance of the neural network, it should be noted that the comparison was made with the project [24] mentioned above, the same dataset was used for comparison, where you can see the improvement of the results obtained from our convolutional neural network on this project since having 3 layers allows a more accurate diagnosis based on the images.

In medicine, sensitivity as stated above is the percentage of true positives that are malignant lesions correctly identified, while specificity measures how many samples predicted as true negatives are actually so. The data shown in Table 3, are the most optimal as they explain the ranking of the improvement of accuracy, sensitivity and precision results.

For future work, we propose the implementation of the Keras tool, since with it we can obtain better results, not only binary, but also classify into various types of cancer once the melanoma has been detected. Using the categorical and non-binary type so that it can load different types of images.

To obtain a better classification, segmentation could be used before image training to improve accuracy when validating the images, for which a U-Net architecture would have to be implemented.

REFERENCES

[1] M. A. Arasi, E.-S. A. El-Dahshan, E.- Sayed, M. El-Horbaty, and A.-B. M. Salem, "Malignant Melanoma Detection Based on Machine Learning Techniques: A Survey," *Egypt. Comput. Sci. J.*, vol. 40, no. 03, pp. 1110–2586, 2016, [Online]. Available: http://www.ecsjournal.org/Archive/Volume40/Issue3/1.pdf.

[2] R. L. Siegel, K. D. Miller, and A. Jemal, "Cancer statistics, 2020," CA. Cancer J. Clin., vol. 70, no. 1, pp. 7–30, Jan. 2020, doi: 10.3322/caac.21590.

[3] R. L. Siegel, K. D. Miller, and A. Jemal, "Cancer statistics, 2019," CA. Cancer J. Clin., vol. 69, no. 1, pp. 7–34, Jan. 2019, doi: 10.3322/caac.21551.

[4] Melanoma Research Foundation (MRF), "Conciencia del melanoma | Fundación de Investigación del Melanoma." https://melanoma.org/melanoma-education/melanoma-awareness/

[5] C. Sordo and C. Gutiérrez, "Cáncer de piel y radiación solar: experiencia peruana en la prevención y detección temprana del cáncer de piel y melanoma," Rev. Perú. Med. Exp. Salud Pública, vol. 30, no. 1, 2014, doi: 10.17843/rpmesp.2013.301.167.

[6] W. Ramos, N. Guerrero, and J. Medina, Análisis de la situación del cáncer en el Perú, 2018, vol. 20, no. 1. 2020.

[7] H. Chang, "Skin cancer reorganization and classification with deep neural network," arXiv, 2017.

[8] M. Goyal, T. Knackstedt, S. Yan, and S. Hassanpour, "Artificial intelligence-based image classification methods for diagnosis of skin cancer: Challenges and opportunities," Comput. Biol. Med., vol. 127, 2020, doi: 10.1016/j.compbiomed.2020.104065.

[9] A. Romero Lopez, X. Giro-I-Nieto, J. Burdick, and O. Marques, "Skin lesion classification from dermoscopic images using deep learning techniques," Proc. 13th IASTED Int. Conf. Biomed. Eng. BioMed 2017, no. January, pp. 49–54, 2017, doi: 10.2316/P.2017.852-053.

[10] Instituto Nacional del Cáncer de los Institutos Nacionales de la Salud de EE. UU., "Tratamiento del cáncer de piel (PDQ®)–Versión para profesionales de salud," cancer.gov, 2020.

[11] J. M. Guilera et al., Comprender el melanoma y otros cánceres de piel: Factores de riesgo. Diagnóstico y tratamiento. Fotoprotección. Claves de autoexploración., 1st editio. Barcelona: Amat editorial, 2015.

[12] P. Castañeda and J. Eljure, "Cancer de piel un problema actual," Artic. Revis., vol. 59, no. 2, pp. 6–14, 2016, [Online]. Available: https://www.medigraphic.com/pdfs/facmed/un-2016/un162b.pdf.

[13] R. Florez and J. Fernandez, "Las Redes Neuronales Artificiales," Netbiblo, 2008. https://books.google.com.pe/books?id=X0uLwi1Ap4QC&printsec=copyright#v=onepage&q&f=false

[14] K. O'Shea and R. Nash, "An Introduction to Convolutional Neural Networks," pp. 1–11, 2015,

[Online]. Available: http://arxiv.org/abs/1511.08458.

[15] J. Torres, "DEEP LEARNING Introducción práctica con Keras," Deep Learning — Aprendizaje profundo, 2018. https://torres-ai.medium.com/deep-learning-aprendizaje-profundo-52084448ea0e

[16] L. Le, Y. Zheng, G. Carneiro, and L. Yang, Deep Learning and Convolutional Neural Networks for Medical Image Computing, Precision Medicine, High Performance and Large-Scale Datasets, 1st ed. Springer International Publishing, 2017.

[17] P. Loncomilla, "Deep learning: Redes convolucionales," 2016.

[18] I. Goodfellow, Y. Bengio, and A. Courville, Deep Learning. Cambridge, MA, USA: The MIT Press, 2016.

[19] D. Wei, B. Zhou, A. Torralba, and W. T. Freeman, "mNeuron: A Matlab Plugin to Visualize Neurons from Deep Models," Massachusetts Institute of Technology. https://donglaiw.github.io/proj/mneuron/index.html

[20] M. Summerfield, Python 3 (Programación). ANAYA MULTIMEDIA, 2009.

[21] U. D. Center, "ISIC Archive," ISIC, 1979. https://www.isic-archive.com

[22] P. FERREIRA, "ADDI - Automatic computer-based Diagnosis system for Dermoscopy Images," 2012. https://www.fc.up.pt/addi/ph2 database.html

[23] L. Fausett, "Fundamentals of Neural Networks Architectures, Algorithms, and Applications." https://dl.matlabyar.com/siavash/Neural Network/Book/Fausett L.-Fundamentals of Neural Networks_ Architectures, Algorithms, and Applications (1994).pdf

[24] A. Romero López, "Skin lesion detection from dermoscopic images using convolutional neural networks," no. January 2017.